High-pressure magnetic study of Fe-Ni and Fe-Pt Invar alloys

L. Nataf,* F. Decremps, and J. C. Chervin
Physique des Milieux Denses, Institut de Minéralogie et Physique des Milieux Condensés, Université Pierre et Marie Curie-Paris 6, CNRS UMR 7590, 140 rue de Lourmel, 75015 Paris, France

O. Mathon and S. Pascarelli
European Synchrotron Radiation Facility, BP 220, 38043 Grenoble Cedex, France

J. Kamarád
Institute of Physics, Academy of Sciences of the Czech Republic (ASCR), Na Slovance 2, 182 21 Prague 8, Czech Republic

F. Baudelet, A. Congeduti, and J. P. Itié
Synchrotron SOLEIL, L'Orme des Merisiers, Saint-Aubin, BP 48, 91192 Gif-sur-Yvette Cedex, France
(Received 17 March 2009; revised manuscript received 4 September 2009; published 6 October 2009)

Magnetic properties of $Fe_{64}Ni_{36}$ and Fe-Pt Invar alloys under high pressure have been investigated through x-ray magnetic circular dichroism (XMCD) up to 12 GPa at ambient temperature and superconducting quantum interference device magnetometer up to 1 GPa for different isotherms, from 10 to 300 K. Results obtained with both techniques on Fe-Pt samples can be well interpreted through the 2γ-state interpretation of the Invar effect. For the $Fe_{64}Ni_{36}$ alloy, the relative evolution of the iron magnetic moment at 300 K, measured through XMCD, shows the existence of a plateau between 4 and 10 GPa, also expected within this approach. In the low-pressure range, the evolution of magnetization indicates that the itinerant character of Fe-Ni alloys may affect the transition.

DOI: 10.1103/PhysRevB.80.134404 PACS number(s): 62.50.−p, 75.50.Bb, 78.70.Dm

I. INTRODUCTION

The Invar effect has been extensively studied since its discovery in 1897.[1] It has been clearly established that the almost zero thermal expansion over a large range of temperature is related to magnetovolumic instabilities which give rise to a reduction in the volume and cancel the expansion due to the lattice vibrations. Besides this peculiar thermal expansion, other physical properties such as heat capacity, elastic modulus, or magnetization show unusual behaviors under temperature. Anomalies are also observed as a function of composition, magnetic field, or pressure, where a very low-pressure derivative of the bulk modulus is observed.[2,3] Up to now, a unique microscopic interpretation of the magnetovolumic effects responsible for the Invar effect is still lacking. Even though a large amount of models have been proposed,[4] Invar specific properties are currently explained through two main models. A localized description, based on the existence of two distinct magnetic states of iron and an itinerant description, based on a continuum of states of iron spin moment. The first one has been initially proposed by Weiss[5] who suggested that an increase in temperature allows a transition from a high-spin (HS) state to a low-spin (LS) state which has a smaller volume. Therefore the lattice expansion is counterbalanced by this transition. Within this interpretation, increasing pressure gives rise to a reduction in the energy difference between the two states up to a transition pressure beyond which the LS state becomes the more favorable configuration. This interpretation has been supported by modern band-structure calculations which give a more detailed picture of the electronic transition.[6–8] These works have shown that the HS to LS transition is actually associated with an electronic transfer from the antibonding majority-spin states of t_{2g} symmetry to the nonbonding minority-spin states of e_g symmetry. Both temperature and pressure evolutions of physical properties are thus expected to present first-order discontinuities. From an experimental point of view, Mössbauer spectroscopy experiments support this model, showing that the LS density increases with temperature[9] or with pressure.[10,11] Nevertheless, some results obtained on Fe-Ni samples are inconsistent with this two-states model. This has led van Schilfgaarde *et al.*[12] to propose a different microscopic interpretation for these alloys. The Invar effect is explained through a volume reduction driven by a continuous transition from a ferromagnetic state to a noncollinear configuration of the spin moment. This *ab initio* model succeed in reproducing experimental data like the magnetic moment evolution with the composition or the low value of the pressure derivative of the bulk modulus and its pressure evolution.[13] Moreover, recent polarized neutron diffraction[14] and spin-polarized electron momentum distributions[15] results are in contradiction with the 2γ-state model. They show that there is no charge transfer between orbitals, the fraction of electrons with e_g symmetry remaining constant over the whole temperature range. According to this approach no first-order discontinuities are expected to occur.

Among Invar alloys, which are essentially Fe-based alloys (for a review, see Ref. 16), Fe-Ni and Fe-Pt are recognized as prototypical. In spite of similar low expansion coefficients, these compounds present different behaviors showing their different magnetic properties. In Fe-Ni samples, deviations from the Vegard and Slater-Pauling laws are observed[17,18] whereas in Fe-Pt samples, lattice constant and magnetic moment evolutions are linear as a function of the composition.[19] This is connected to the itinerant (Fe-Ni) and localized (Fe-

Pt) character of the magnetism. Moreover, both iron and nickel are responsible for the magnetism in Fe-Ni whereas platinum magnetism is induced by the orbitals hybridization with iron. As the investigation of the pressure effect on the magnetic properties of 3*d* transition metals can provide a better understanding of the itinerant magnetism, many studies have been previously focused on the magnetic properties of Invar compounds. As already mentioned, Mössbauer spectroscopy measurements under pressure have given experimental evidence of the HS to LS transition.[10,11,20] The pressure evolution of x-ray magnetic circular dichroism (XMCD) spectra observed on $Fe_{72}Pt_{28}$ (Ref. 21) and XES spectra on $Fe_{64}Ni_{36}$,[22] where both techniques are sensitive to the magnetic moment, have been well interpreted within the 2γ-state framework. On the other hand, recent ac susceptibility results on $Fe_{64}Ni_{36}$ show a continuous magnetic phase transition[23] which supports the noncollinear interpretation.

A previous structural study performed at 30 K, through x-ray diffraction has shown that, for both samples, the pressure dependence of the cell volume can be satisfactorily fitted using a "Weiss-like equation of state." Nevertheless the interpretation of the $Fe_{64}Ni_{36}$ compound is less straightforward and suggests that other equations of state may be suitable. This different high-pressure behavior of the cell volume led us to investigate the magnetic properties of Fe-Ni and Fe-Pt samples under pressure. In this paper XMCD experiments at ambient temperature performed on $Fe_{64}Ni_{36}$ and $Fe_{72}Pt_{28}$ samples up to 12 GPa are reported. This technique is very useful to investigate magnetic properties of 3*d* transition metals, thanks to its element and orbital selectivity and to its sensitivity to very small magnetic moments. The aim of this study was to elucidate whether or not the magnetic moment has a continuous evolution with pressure in order to test which model is the most suitable to interpret Invar behavior. Moreover Fe-Ni and Fe-Pt alloys present different magnetic properties and evolutions with pressure, in particular, in the low-pressure range. In order to obtain a direct and precise determination of the magnetic moment under hydrostatic pressure, we have performed magnetization measurements with a superconducting quantum interference device (SQUID) magnetometer on both samples, up to 1 GPa on different isotherms (from 10 to 300 K).

II. EXPERIMENTAL PROCEDURE

A. XMCD experiments

For XMCD experiments, the samples shape was a disk of diameter 30 μm and thickness around 5 μm, extracted from polycrystalline rods. Samples were annealed for one day in an argon atmosphere at 800 °C to remove residual stress. The densities have been measured [$\rho_{Fe_{64}Ni_{36}}=8.078(5)$ g/cm^3 and $\rho_{Fe_{72}Pt_{28}}=11.973(5)$ g/cm^3] and found close to those of single-crystal values.[25,26] Moreover these samples have been characterized and investigated in previous studies[3,21,24] and the XAS spectrum (shown in Fig. 1 for the Fe-Ni case) presents the fcc symmetry signature, as expected. The samples were placed into a Cu-Be membrane diamond-anvil cell,[27] filled with a methanol-ethanol (4:1) mixture as pressure medium. A ruby ball[28] was also loaded close to the sample in order to determine the pressure, thanks to the fluorescence method.[29]

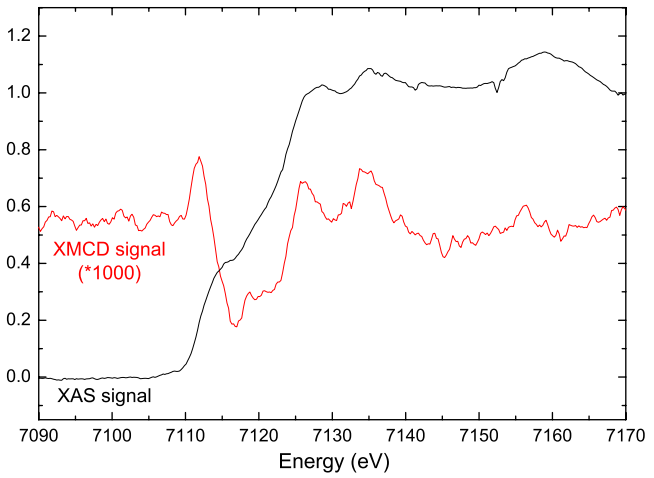

FIG. 1. (Color online) Normalized XAS and XMCD signals of $Fe_{64}Ni_{36}$ at 0.38 GPa.

XMCD and XAS spectra, shown in Fig. 1 for the Fe-Ni case, were recorded at the European Synchrotron Radiation Facility at the energy dispersive XAS beamline ID24 (Ref. 30) which allows the detection of *K*-edge XMCD signals of 3*d* transition metals under pressure.[31] A magnetic field of 0.4 T was applied to the sample environment in the direction of x-ray propagation. Each XMCD spectrum was obtained by accumulating 500 to 1500 XAS spectra, inverting the magnetic field between two successive XAS spectra. It should be reminded here that XMCD measures the projection of the magnetic moment on the x-ray propagation axis. The quantity measured through XMCD is proportional to the spin and orbital moment carried by the probed electronic level of the transition.

Many theoretical studies, using different approaches,[32–36] have been dedicated to the interpretation of the XMCD signal measured at the *K* edge (which probes the 4*p* empty states) of transition metals. Still, its precise origins are not fully understood. Nevertheless, all these works lead to the conclusion that the main contribution is due to interaction of the excited 4*p* photoelectrons with the spin-polarized 3*d* bands of the neighboring atoms. Therefore, one can conclude that the XMCD integral is proportional to the orbital magnetic moment of the 3*d* bands.

B. SQUID experiments

For these experiments, performed at the Institute of Physics, Academy of Sciences of the Czech Republic, a nonmagnetic Cu-Be hydrostatic cell, recently developed for magnetization measurements,[37] was used. The same $Fe_{64}Ni_{36}$ sample and a Fe_3Pt polycrystalline sample were investigated. The samples were loaded into the cell filled with spindle oil (OL3) as pressure medium. The *in situ* pressure is determined at low temperature, thanks to the superconducting transition of a Pb ball whose critical temperature shifts with pressure. Using a SQUID magnetometer (Quantum Design

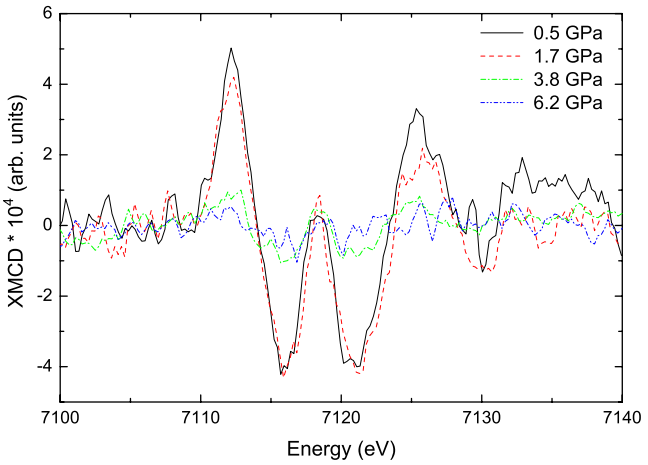

FIG. 2. (Color online) Normalized XMCD signals obtained on the $Fe_{72}Pt_{28}$ sample, at 0.5 GPa in black solid line, 1.7 GPa in red dashed line, 3.8 GPa in green dotted line, and 6.2 GPa in blue dot-dashed line.

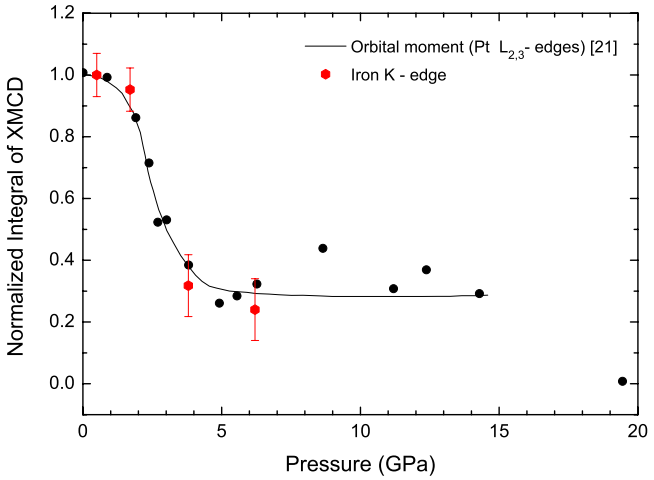

FIG. 3. (Color online) Pressure dependence of normalized integrals of XMCD signals for the $Fe_{72}Pt_{28}$ sample. Red diamonds: Fe K edge and black circles: orbital magnetic moment deduced from the measurements at the Pt $L_{2,3}$ edges (Ref. 21).

MPMS-5S), the magnetization per atom of both alloys under pressure and as a function of temperature were measured, in an external magnetic field of 4 T.

III. RESULTS AND DISCUSSION

A. Fe-Pt

The XMCD signal collected on the $Fe_{72}Pt_{28}$ sample (Fig. 2) is in good agreement with those measured by Ståhler *et al.*[38] Since the intensity of the transmitted beam at the Fe K edge is weakened not only by the diamonds, but also by the absorption of Pt, each XMCD spectrum was obtained using integration times between 8 and 24 h (depending on the pressure), in order to obtain a sufficient signal-to-noise ratio.

The pressure dependence of the normalized integral of XMCD signals obtained at the Fe K edge on $Fe_{72}Pt_{28}$ is plotted in Fig. 3 (red diamonds). The orbital magnetic moment of platinum deduced from the experiment at the Pt $L_{2,3}$ edges[21] is also represented in this figure (black line). It has to be noted that a magnetic moment still exists at high pressure (6 GPa), which has also been observed by pulsed magnetic field measurements.[39] One can observe a clear and abrupt decrease in the pressure evolution of both the spectra (shown in Fig. 2) and the normalized integrals of XMCD between 1.7 and 3.8 GPa (Fig. 3, red diamonds). In these alloys, magnetism is due to Fe, and hybridization of Fe 3d bands and Pt 5d bands is responsible for the presence of a magnetic moment on Pt. As already mentioned, the integral of the XMCD signal at the K edge is proportional to the 3d-orbital magnetic moment. The good superposition of results at the Fe K edge and at the Pt $L_{2,3}$ indicates that the magnetic moment of both iron and platinum atoms behaves similarly. Therefore our results support the conclusion proposed by Odin *et al.*: the abrupt decrease in the magnetic moment with pressure corresponds to the HS to LS transition and therefore provides another evidence of the two-states model for the Fe-Pt alloys.

Figure 4 presents the magnetization as a function of pressure of the Fe-Pt sample at different temperatures. At 10 K, the average magnetic moment per atom, $2.02\mu_B$, corresponds to previous measurements on Fe-Pt samples.[40,41] The relative magnetization $M(T,p)/M(T,0)$ at ambient temperature is in very good agreement with Matsushita *et al.*[39] results [at about 1 GPa, we observe a value of 0.32 compared with 0.4 (Ref. 39)]. The Curie temperature T_C of the sample is 335 K at ambient pressure and decreases strongly with increasing pressure (as clearly shown in Fig. 5). The pressure parameter $dT_C/dp = -52.4 \pm 0.6$ K/GPa has been determined from $M(T,p,100\ \mathrm{G})$ curves. Therefore at 300 K, the ferromagnetic to paramagnetic transition induced by pressure is the main reason for the magnetic moment decrease. At 200 K,

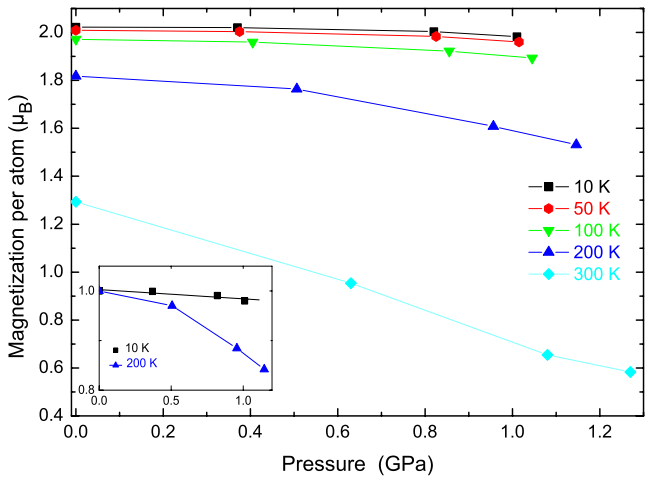

FIG. 4. (Color online) Pressure dependence of the magnetization per atom (with an external magnetic field of 4 T) of the Fe_3Pt sample at different temperature: 10 K in black squares, 50 K in red circles, 100 K in green down triangles, 200 K in blue up triangles, and 300 K in cyan diamonds. Inset: normalized value of the magnetization with pressure $M(T,p)/M(10,0)$ at 10 and 200 K (same symbols).

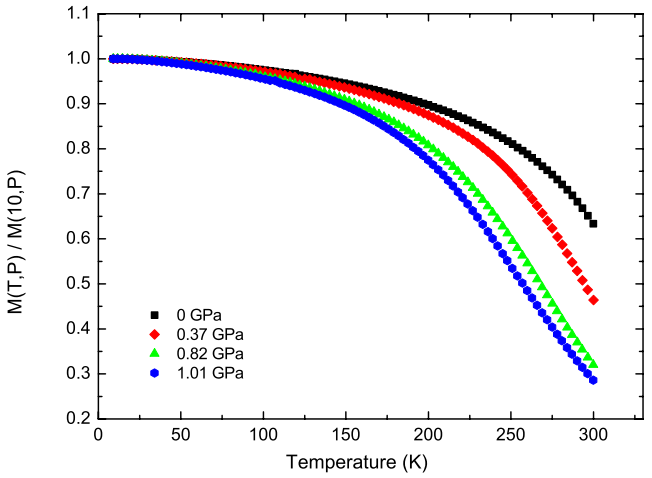

FIG. 5. (Color online) Temperature dependence of the magnetization per atom of the Fe_3Pt sample at different pressures. Each curve has been normalized to the 10 K value of the magnetization: 0 GPa in black squares, 0.37 GPa in red diamonds, 0.82 GPa in green triangles, and 1.01 GPa in blue circles.

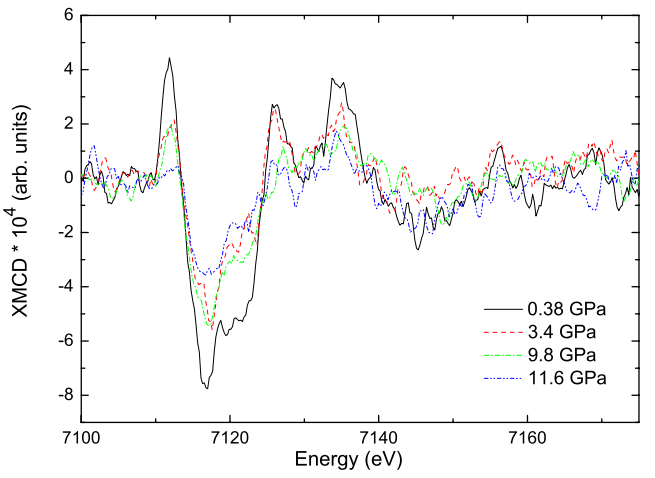

FIG. 6. (Color online) Normalized XMCD signals obtained on the $Fe_{64}Ni_{36}$ sample, at 0.4 GPa in black solid line, 3.4 GPa in red dashed line, 6.9 GPa in green dotted line, and 11.6 GPa in blue dot-dashed line.

the magnetization shows a clear decrease with pressure, more pronounced above 0.5 GPa. But for this temperature, one has to take into account the typical flattening of the magnetization (Fig. 5) which may be partially responsible for the magnetization reduction observed above 0.5 GPa. For the lower temperatures (from 100 to 10 K), a smoother reduction with pressure of the magnetization is observed (with a pressure coefficient of $\partial \ln M / \partial p = -0.02$ GPa^{-1}). In these cases the Curie temperature is not reached even at the highest pressure. This magnetization evolution is then due to the electronic transition from the high-spin state to the low-spin one induced by the pressure. Although the pressure also induces a transition to the paramagnetic state in the case of our sample, these results are in good agreement with a previous study[42] and can be interpreted within the 2γ-state model framework.

B. Fe-Ni

The evolution of the XMCD spectra under pressure measured on the $Fe_{64}Ni_{36}$ sample is shown in Fig. 6. The main specific peaks and their energy positions correspond to the spectra obtained by Gofron *et al.*[43] on three different Fe-Ni alloys. As seen in Fig. 6 the XMCD intensity decreases with pressure, in particular, between 0.4 and 3.4 GPa. This decrease is emphasized by the signal integrals whose pressure dependence is given in Fig. 7. The XMCD signal then remains constant up to 10 GPa (within the error bar). Above 10 GPa, the decrease in the magnetic moment is more evident and there is no doubt that the magnetic moment will vanish at higher pressure. The nonmagnetic state has been actually measured on a $Fe_{64}Ni_{36}$ polycrystalline sample around 15 GPa, by x-ray emission spectroscopy,[22] and on pure Fe (Ref. 44) and Fe_3C (Ref. 45) by XMCD.

Here again, the magnetic moment evolution with pressure can be interpreted through the two states description. Starting from a mixed configuration of HS and LS states at ambient pressure and temperature, the LS state becomes more stable, thus more populated, than the HS one as the pressure is increasing (in the 0–3 GPa range). Once all the electrons are in the LS state, the XMCD intensity reflects only the LS state and remains constant (between 4 and 10 GPa), up to the transition into the nonmagnetic state.

On the contrary, the noncollinear model which predicts a smooth and continuous decrease in the magnetic moment under pressure, fails to reproduce this result. The existence of a plateau, which is absolutely significant, was also found by Rueff *et al.*[22] at the same relative intensity and supports the two-states model, even for the Fe-Ni compounds. This conclusion is in good agreement with a previous ultrasonics measurements performed on the same $Fe_{64}Ni_{36}$ sample at ambient temperature.[3]

Through Mössbauer spectroscopy, the Curie temperature T_C is found to decrease strongly with pressure ($dT_C/dp = -44$ K/GPa) in such a way that T_C is predicted to be equal to room temperature around 7 GPa.[10] Nevertheless, XMCD

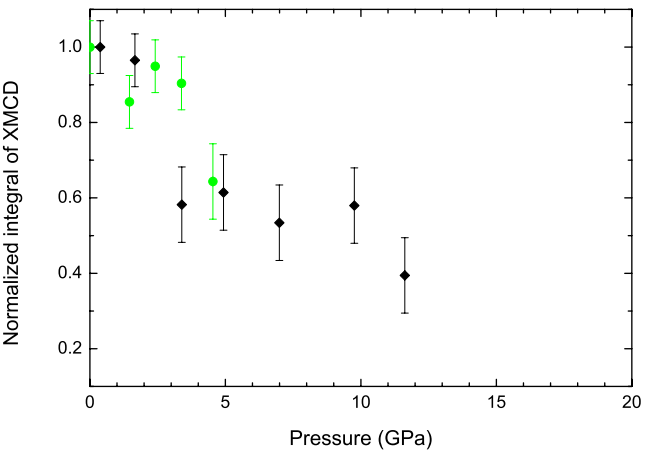

FIG. 7. (Color online) Pressure dependence of normalized integrals of XMCD signals for the $Fe_{64}Ni_{36}$ sample. Black diamonds and green circles correspond to different runs.

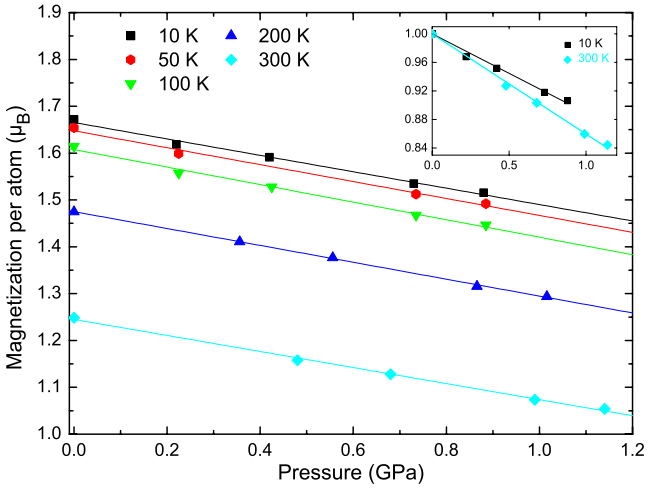

FIG. 8. (Color online) Pressure dependence of the magnetization per atom (with an external magnetic field of 4 T) of the $Fe_{64}Ni_{36}$ sample at different temperature: 10 K in black squares, 50 K in red circles, 100 K in green down triangles, 200 K in blue up triangles, and 300 K in cyan diamonds. Inset: normalized value of the magnetization with pressure $M(T,p)/M(10,0)$ at 10 and 300 K (same symbols).

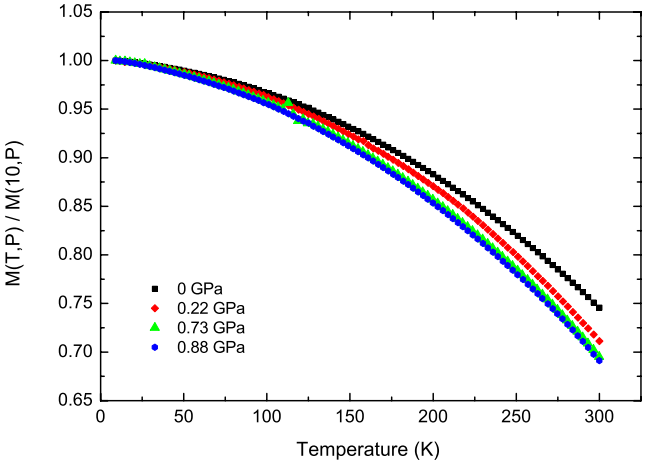

FIG. 9. (Color online) Temperature dependence of the magnetization per atom of the $Fe_{64}Ni_{36}$ sample at different pressures. Each curve has been normalized to the 10 K value of the magnetization: 0 GPa in black squares, 0.22 GPa in red diamonds, 0.73 GPa in green triangles, and 0.88 GPa in blue circles.

signals can be measured up to these pressures and even higher, indicating that the sample is still ferromagnetic, otherwise no XMCD signal would be detected. This observation points out to a contradiction, which may be explained taking into account the sample history. Indeed, time and temperature of annealing play a crucial role in the magnetic properties of Invar alloys. In particular Wei *et al.*[46] have found a clear dependence of T_C and dT_C/dp with the annealing procedure.

At ambient pressure and at 10 K, the magnetization of the $Fe_{64}Ni_{36}$ alloy is found to be $1.66\mu_B$ in very good agreement with previous measurements.[47] As seen in Fig. 8 where SQUID results are reported, the pressure dependence of the magnetization is not strongly affected by the temperature. Whatever the temperature, the decrease in the magnetization is linear with a similar slope ($\partial \ln M/\partial p = -0.11$ GPa^{-1} at 10 K and $\partial \ln M/\partial p = -0.14$ GPa^{-1} at 300 K). The inset of Fig. 8, which represents the relative value of the magnetization, points out the extraordinary decrease in the magnetization with pressure in the FeNi alloy, in comparison with the standard small decrease (of about $\partial \ln M/\partial p = -0.03$ GPa^{-1}, in FePt or in pure iron or nickel). This result does not correspond to what has been previously measured by Hayashi *et al.*[42] This different behavior may be explained by a different history or composition of the sample. In the FeNi samples, the Curie temperature is higher than in FePt ones (520 K with respect to 335 K) and as it can be seen in Fig. 9, the temperature of the sample remains well below T_C on the whole pressure range. Thus in this case, a transition to the paramagnetic state cannot be responsible for the observed pressure behavior (Fig. 8).

As mentioned in Sec. I, the interpretation of results for Fe-Ni alloys has always been more debated than for Fe-Pt, from both the experimental and theoretical point of views. The XMCD results are consistent with a transition from a mixed HS/LS state to a pure LS state induced by pressure. On the other hand, in the two-state model, the pressure dependence of the magnetization should be affected by the temperature, as observed in the FePt sample. This is not the case in this low-pressure range ($p < 1$ GPa), the results showing a very similar slope with pressure in the whole explored temperature range (Fig. 8). However, it must be noted that in the case of itinerant magnets, the magnetic transition is much more sensitive to pressure than to temperature, since the temperature range is well below T_C.[10] Moreover, the XMCD technique provides a local and selective probe of the Fe magnetic moment, whereas SQUID measurements provide an average magnetic moment of the investigated sample.

In any case, the present magnetization results (Fig. 8) lead to the need of an extension of the two-state model in the low-pressure range. Besides the HS to LS transition, one may have to consider an additional contribution, which is difficult to evaluate precisely within the present theories framework but could be attributed to intermediate magnetic states.[48]

IV. CONCLUSION

Ambient temperature results from x-ray magnetic circular dichroism lead to similar conclusions for both samples. The pressure dependence of the magnetic moment cannot be interpreted within the noncollinear framework, since a plateau occurs between 4 and 10 GPa, the existence of which is not expected in a noncollinear picture. In fact the results obtained on the Fe-Pt sample (through XMCD and SQUID techniques) can be interpreted through the 2γ-state model at all temperatures investigated. Whereas the Fe-Ni alloys behavior is more complex and its interpretation seems to require both models according to the temperature. Indeed, ambient temperature measurements of the bulk modulus[3] and of the magnetization[49] show linear evolutions with pressure

with an abrupt change in slope, around 3 GPa, in contradiction with the noncollinear interpretation. On the other hand, the temperature independence of the e_g electronic population[14] is not expected by the 2γ-state model and the pressure behavior of the magnetization observed through SQUID measurements may require both points of view. Therefore, it would be of great interest to perform XMCD or ultrasonics experiments under pressure at low temperature on the peculiar case of Fe-Ni alloys, for which the origin of Invar anomalies appears to be much more complex to explain than for the Fe-Pt compounds.

ACKNOWLEDGMENTS

The authors would like to acknowledge M. M. Abd-Elmeguid and A. Polian for fruitful comments and suggestions.

*lucie.nataf@unican.es

[1] C. E. Guillaume, C. R. Acad. Sci. **125**, 235 (1897).
[2] Ll. Mañosa, G. A. Saunders, H. Rahdi, U. Kawald, J. Pelzl, and H. Bach, Phys. Rev. B **45**, 2224 (1992).
[3] F. Decremps and L. Nataf, Phys. Rev. Lett. **92**, 157204 (2004).
[4] E. F. Wassermann, J. Magn. Magn. Mater. **100**, 346 (1991).
[5] R. J. Weiss, Proc. Phys. Soc. **82**, 281 (1963).
[6] V. L. Moruzzi, Phys. Rev. B **41**, 6939 (1990).
[7] M. Podgórny, Phys. Rev. B **46**, 6293 (1992).
[8] P. Entel, E. Hoffmann, P. Mohn, K. Schwarz, and V. L. Moruzzi, Phys. Rev. B **47**, 8706 (1993).
[9] Y. Kong, F. S. Li, M. Kaack, J. Pelzl, P. Stauche, and H. Bach, J. Phys.: Condens. Matter **12**, 2079 (2000).
[10] M. M. Abd-Elmeguid and H. Micklitz, Physica B (Amsterdam) **161**, 17 (1989).
[11] M. M. Abd-Elmeguid, B. Schleede, and H. Micklitz, J. Magn. Magn. Mater. **72**, 253 (1988).
[12] M. van Schilfgaarde, I. A. Abrikosov, and B. Johansson, Nature (London) **400**, 46 (1999).
[13] L. Dubrovinsky, N. Dubrovinskaia, I. A. Abrikosov, M. Vennström, F. Westman, S. Carlson, M. van Schilfgaarde, and B. Johansson, Phys. Rev. Lett. **86**, 4851 (2001).
[14] P. J. Brown, K. U. Neumann, and K. R. A. Ziebeck, J. Phys.: Condens. Matter **13**, 1563 (2001).
[15] J. W. Taylor, J. A. Duffy, A. M. Bebb, J. E. McCarthy, M. R. Lees, M. J. Cooper, and D. N. Timms, Phys. Rev. B **65**, 224408 (2002).
[16] A. P. Wohlfarth, J. Magn. Magn. Mater. **10**, 120 (1979).
[17] M. Shiga, IEEE Trans. Magn. **8**, 666 (1972).
[18] Y. Nakamura, IEEE Trans. Magn. **12**, 278 (1976).
[19] K. Sumiyama, M. Shiga, and Y. Nakamura, J. Magn. Magn. Mater. **31-34**, 111 (1983).
[20] M. M. Abd-Elmeguid, Nucl. Instrum. Methods Phys. Res. B **76**, 159 (1993).
[21] S. Odin, F. Baudelet, Ch. Giorgetti, E. Dartyge, J. P. Itié, A. Polian, J. C. Chervin, S. Pizzini, A. Fontaine, and J. P. Kappler, Europhys. Lett. **47**, 378 (1999).
[22] J. P. Rueff, A. Shukla, A. Kaprolat, M. Krisch, M. Lorenzen, F. Sette, and R. Verbeni, Phys. Rev. B **63**, 132409 (2001).
[23] M. Matsushita, Y. Miyoshi, S. Endo, and F. Ono, Phys. Rev. B **72**, 214404 (2005).
[24] L. Nataf, F. Decremps, M. Gauthier, and B. Canny, Phys. Rev. B **74**, 184422 (2006).
[25] P. Renaud, Ph.D. thesis, Université de Lausanne, 1988.
[26] G. Hausch, J. Phys. F: Met. Phys. **6**, 1015 (1976).
[27] J. C. Chervin, B. Canny, J. M. Besson, and Ph. Pruzan, Rev. Sci. Instrum. **66**, 2595 (1995).
[28] J. C. Chervin, B. Canny, and M. Mancinelli, High Press. Res. **21**, 305 (2002).
[29] H. K. Mao, J. Xu, and P. M. Bell, J. Geophys. Res. **91**, 4673 (1986).
[30] S. Pascarelli, O. Mathon, and G. Aquilanti, J. Alloys Compd. **362**, 33 (2004).
[31] O. Mathon, F. Baudelet, J. P. Itié, S. Pasternak, A. Polian, and S. Pascarelli, J. Synchrotron Radiat. **11**, 423 (2004).
[32] H. Ebert, P. Strange, and B. L. Gyorffy, J. Appl. Phys. **63**, 3055 (1988).
[33] G. Y. Guo, Phys. Rev. B **55**, 11619 (1997).
[34] C. Brouder and M. Hikam, Phys. Rev. B **43**, 3809 (1991).
[35] J. I. Igarashi and K. Hirai, Phys. Rev. B **53**, 6442 (1996).
[36] O. Šipr and H. Ebert, Phys. Rev. B **72**, 134406 (2005).
[37] J. Kamarád, Z. Machátová, and Z. Arnold, Rev. Sci. Instrum. **75**, 5022 (2004).
[38] S. Stähler, M. Knülle, G. Schütz, P. Fischer, S. Welzel-Gerth, and B. Buchholz, J. Appl. Phys. **73**, 6063 (1993).
[39] M. Matsushita, T. Nishimura, S. Endo, M. Ishizuka, K. Kindo, and F. Ono, J. Phys.: Condens. Matter **14**, 10753 (2002).
[40] O. Caporaletti and G. M. Graham, J. Magn. Magn. Mater. **22**, 25 (1980).
[41] D. Paudyal, T. Saha-Dasgupta, and A. Mookerjee, J. Phys.: Condens. Matter **16**, 2317 (2004).
[42] K. Hayashi and N. Mori, Solid State Commun. **38**, 1057 (1981).
[43] K. J. Gofron, C. W. Kimball, G. Jennings, P. L. Lee, and P. A. Montano, J. Phys. IV 7– **C2**, 421 (1997).
[44] O. Mathon, F. Baudelet, J. P. Itié, A. Polian, M. d'Astuto, J. C. Chervin, and S. Pascarelli, Phys. Rev. Lett. **93**, 255503 (2004).
[45] E. Duman, M. Acet, E. F. Wassermann, J. P. Itié, F. Baudelet, O. Mathon, and S. Pascarelli, Phys. Rev. Lett. **94**, 075502 (2005).
[46] S. Wei, R. Duraj, R. Zach, M. Matsushita, A. Takahashi, H. Inoue, F. Ono, H. Maeta, A. Iwase, and S. Endo, J. Phys.: Condens. Matter **14**, 11081 (2002).
[47] G. Dumpich, J. Kästner, U. Kirschbaum, H. Mühlbauer, J. Liang, T. Lübeck, and E. F. Wassermann, Phys. Rev. B **46**, 9258 (1992).
[48] I. A. Abrikosov, A. E. Kissavos, F. Liot, B. Alling, S. I. Simak, O. Peil, and A. V. Ruban, Phys. Rev. B **76**, 014434 (2007).
[49] S. Endo, J. Yamada, S. Imada, M. Ishizuka, K. Kindo, and S. Miyamoto, Rev. Sci. Instrum. **70**, 2445 (1999).